Fermi National Accelerator Laboratory

FN-343
8000.000

Long Time Simulations of the Beam - Beam Interaction

David Neuffer, Alan Riddiford and Alessandro Ruggiero

July 1981

In previous papers[1,2] we have presented results of "long-time" simulations of the beam-beam interaction at parameters corresponding to $\bar{p}p$ colliders. These investigations are undertaken to search for evidence of long-time scale instability such as "Arnold Diffusion" in $\bar{p}p$ colliders. Previously we chose tunes near resonances for these investigations. In reference 1, we presented results of simulations of 60 million turns (20 $\bar{p}p$ "Tevatron" minutes) for two cases: Case A: $\nu_x = .245$, $= \nu_y = .245$, $\Delta\nu = .01$ near the 1/4, 1/4 resonance and Case B: $\nu_x = .245$, $= \nu_y = .12$, $\Delta\nu = .01$ near the 1/4, 1/8 resonance (ν_x and ν_y are horizontal and vertical betatron tunes, $\Delta\nu$ the beam-beam tune shift). We saw no evidence for a long-time instability.

In this paper we extend these cases (A and B) for an additional 60 million turns. We also present results of a third case (C) chosen with tunes free of resonances up to 9th order: $\nu_x = .3439$, $\nu_y = 0.1772$, $\Delta\nu = .01$. Results of repeatability experiments for cases A, B, and C are presented. Evidence for nonrepeatability is shown in case B. Limits of rms emittance growth for all three cases are presented and no evidence for long-time instability is shown.

I. Equations of Motion and Simulation Procedure

The simulation procedure is basically the same as that in reference 1. The equations of motion of particles are:

$$x'' + K_x(s)\, x = \frac{-4\pi\Delta\nu_x}{\beta_x^*} \quad F(x,y)\, \delta_p(s) \cdot x$$

$$y'' + K_y(s)\, y = \frac{-4\pi\Delta\nu_y}{\beta_y^*} \quad F(x,y)\, \delta_p(s) \cdot y \qquad (1)$$

where the various parameters are defined in reference 1. The functions $K_x(s)$, $K_y(s)$ are the alternating gradient focussing functions of an accelerator ring. Transport around the ring can be simulated by a linear matrix found from these functions:

$$\begin{pmatrix} x \\ x' \end{pmatrix}_{\text{final}} = \begin{bmatrix} \cos 2\pi\nu & \beta_x \sin 2\pi\nu \\ -(\beta_x)^{-1} \sin 2\pi\nu & \cos 2\pi\nu \end{bmatrix} \begin{bmatrix} x \\ x' \end{bmatrix}_{\text{initial}} \qquad (2)$$

The terms on the right of equation (1) stand for beam-beam interaction. We use the "weak-strong" approximation, which means $F(x,y)$ is unchanged from turn-to-turn, and in these simulations we have used:

$$F(x,y) = \left(\frac{1. - e^{-\frac{(x^2 + y^2)}{2\sigma^2}}}{\frac{x^2 + y^2}{2\sigma^2}} \right) \qquad (3)$$

which implies a round "strong" Gaussian beam of rms radius σ. We have also used the zero-length approximation, which means the beam-beam interaction is simulated by a kick after each transport around the ring:

$$\begin{pmatrix} x \\ x' \end{pmatrix}_{\text{final}} = \begin{pmatrix} 1 & 0 \\ \dfrac{-4\pi\Delta\nu_x \, F(x,y)}{\beta_x^*} & 1 \end{pmatrix} \begin{pmatrix} x \\ x' \end{pmatrix}_{\text{initial}} \tag{4}$$

In the simulations a set of 100 particles are generated randomly and, as described in reference 1, transported following the matrices (2) and (4). Every 2000 turns the rms emittances X, Y, and R are calculated using:

$$\begin{aligned} X &= 6\sqrt{\langle(x-\bar{x})^2\rangle \langle(x'-\bar{x}')^2\rangle} \\ Y &= 6\sqrt{\langle(y-\bar{y})^2\rangle \langle(y'-\bar{y}')^2\rangle} \\ R &= \sqrt{X^2 + Y^2} \end{aligned} \tag{5}$$

and changes in these values as functions of time are followed.

The parameters σ, β^* are chosen to simulate $p\bar{p}$ collisions in the Fermilab "Tevatron I" project ($\beta^* = 2$ m, $\sigma = .0816$mm) and the other assumptions of the simulations are chosen to approximate $p\bar{p}$ collision conditions.

In these simulations 60 million turns corresponds to 20 minutes Tevatron time in which 30,000 emittance values are generated and analyzed statistically as described below.

The statistical analysis varies in detail from reference 1, since in that run the emittances were grouped and analyzed in sets of 1000 corresponding to individual computer runs and these analyses were combined for analysis of the full 20 minutes.

In Case C all intermediate values are retained and can be analyzed as a whole or grouped as in reference 1. The two methods yield identical results, indicating the accuracy of the combination technique described in reference 1.

II. A Long-time Simulation at Resonance Free Tunes: Case C

($\nu_x = 0.3439$, $\nu_y = 0.1772$, $\Delta\nu = .01$)

Previous long-time simulations have contained large 1/4 and 1/8 resonances, because of our expectation that instability effects are largest near resonances. Accelerators are run at nonresonant tunes to avoid such instability effects. To approximate possible operating conditions more closely and to explore the dependence of long-time instability on the presence of low order resonances, we have undertaken a long-time simulation at resonant free tunes: Case C. The results of that simulation are described in this section.

The tunes for Case C were found by a search for a resonant-free region in tune space.

Figure 1 shows the resonance lines which cross the area in tune space used by Case C. There are no lines of lower than 9th order. There are three 9th order lines, three 10th, two 11th, three 12th and four 13th order lines.

Figure 2 shows the limits of Case C area in tune space, and how close it comes to the undesirable lines of order 3,6, and 8.

The values $\nu_x = 0.3439$ and $\nu_y = 0.1772$ were decided as follows. The distance between a point (X, Y) and a line $AX + BY + C = 0$ is

$$D = \frac{|AX_1 + BY_1 + C|}{\sqrt{A^2 + B^2}} \tag{6}$$

The distance between the three corners (Z_1, Z_2, Z_3) and the nearby sixth, eighth, and third order lines shown in figure 2 are set equal. Defining (X_1, Y_1) as the corner closest to the 8th order line the distances to the lines shown in Figure 2 are

$$D6 = \frac{2X_1 - Y_1 - 0.52}{\sqrt{5}} \tag{7}$$

$$D8 = \frac{-3X_1 - 5Y_1 + 2}{\sqrt{34}} \qquad D3 = \frac{-X_1 + 2Y_1 - 0.02}{\sqrt{5}}$$

This obtains $X_1 = Y_1 + \frac{1}{6}$

$$\text{and} \qquad Y_1 = \frac{8048 - \sqrt{170}}{42900} \tag{8}$$

or

$$X_1 = 0.3539617, \quad Y_1 = 0.1872951 \tag{9}$$

The numbers were truncated to four digits, obtaining:

$$X = 0.3539, \quad Y = 0.1872$$

which moves the (X,Y) corner away from the 8th order line as can be seen in Figure 2.

Figure 3 shows three "bars", sets of 100 consecutive emittance values, for X, Y and R emittance. The straight line best fit for each X-bar does not seem to have the opposite slope of the Y-bar line. So for Case C there does not seem to be an exchange of emittance from X to Y and vice versa.

However, the magnitude of the variation of emittance values is much smaller than in Case A or Case B. Considering the three bars shown in Figure 3 (and the relevant three bars for Case A and Case B) the variation (maximum R emittance value minus the minimum R value) divided by the average value is only 5%.

	Emittance variation/average emittance
Case A	25%
Case B	20%
Case C	5%

Table I gives cumulative emittance averages and doubling times which can be compared with similar tables[1] for cases A and B.

"Doubling" times for X, Y and R emittance are obtained from the slopes of the best straight line fits for X, Y and R as functions of time from t = 0, using rms emittance values calculated every 2000 turns.

The straight line fit of the X-emittance values can be written[3] as

$$X = \bar{X} + b\,(t - \bar{t}\,) \tag{10}$$

where

$$\bar{X} = \frac{1}{N} \Sigma\, x_i \tag{11}$$

$$\bar{t} = \frac{1}{N} \Sigma\, t_i \tag{12}$$

$$b = \frac{1}{DEN} \left[\frac{1}{N} \Sigma\, x_i t_i - \bar{X}\,\bar{t} \right] \tag{13}$$

$$DEN = \frac{1}{N} \Sigma\, t_i^2 - \bar{t}^2 \tag{14}$$

$$SX^2 = \frac{1}{N-2} \Sigma \left[X_i - \bar{X} - b\,(t_i - \bar{t}) \right]^2$$

$$= \frac{1}{1-2/N} \left[\frac{1}{N} \Sigma\, X_i^2 - \bar{X}^2 + b^2 \left(\frac{1}{N} \Sigma\, t_i^2 - \bar{t}^2 \right) - 2b \left(\frac{1}{N} \Sigma\, X_i t_i - \bar{X}\,\bar{t} \right) \right] \tag{15}$$

Using (14) to replace the first parentheses and (13) the second, we obtain $b^2DEN - 2b^2DEN$ so that

$$SX^2 = \frac{1}{1-2/N} \left[\frac{1}{N} \Sigma\, X_i^2 - \bar{X}^2 - b^2 DEN \right] \tag{16}$$

where SX is defined as the "scatter value" and shows no significant growth or decay in time.

The calculated slopes have a statistical error associated with the scattering of the points X_i, which is given by

$$\sigma_b^2 = \frac{SX^2}{N \cdot DEN} \tag{17}$$

A slope b is considered significantly different from zero if it is greater than σ_b in magnitude. A "doubling" time T_x is obtained from b by

$$T_x = \frac{\bar{X}}{b} \tag{18}$$

A negative doubling time is obtained if $b<0$; that is, X is decreasing.

In figures 4,5 and 6 the doubling times T_x, T_y, T_R are compared with T_σ "statistically significant doubling times", found using:

$$T_{\sigma_x} = \pm \frac{\bar{X}}{\sigma_b}$$

Thus, points inside the parabolic-like T_σ lines are statistically different from zero.

Figures 4,5 and 6 show the cumulative doubling times calculated after each of 300 evenly spaced times compared with the statistically significant doubling times. There does not seem to be any indication of a statistically significant non-zero slope.

Figure 7 shows the repeatability results.

Four points were chosen ($x = 0.5\sigma$, 1.0σ, 1.5σ, 2σ; $y=0$; $x'=0$, $y' = 0.1559$ mrad) and transported 60 million turns forward and then backward (time reversed) so that initial and final coordinates can be compared. Agreement is found to 14 digits, as was found for cases A and B in reference 1.

Figure 8 shows 400 points in (x,x') phase space for each of the four orbits used in the repeatability run.

Figure 9 shows 41 orbits in (x,x') phase space: $x = 0.03, 0.06, \ldots, 1.20$ and $x = 0.17$mm $x' = y = 0$ and $y' = 0.1559$ mr for all initial coordinates.

Figure 10 shows 40 orbits in (x,x') phase space with $x = 0.03, 0.06, \ldots, 1.20$; $x' = y' = 0$, $y = \sigma$ for all initial coordinates.

III. Continuation of Cases A and B

To set further limits on possible "Arnold Diffusion", the simulations "A" and "B" of reference 1 have been extended for an additional 60 million turns to a total of 120 million (40 minutes Tevatron 1 time).

Case A has $\nu_x = \nu_y = .245$ and $\Delta\nu = .01$ and shows no significant change in rms emittance in the "twenty minute" simulation of reference 1. Table III and Figure 11 display data from that simulation extended to "forty minutes" in the present results. After 120 million turns we see emittance doubling times of greater than 100 days which are statistically equivalent to zero changes. This confirms the results of reference 1 which show long-time stability in this case.

The repeatability tests of reference 1 have been extended to include 8 orbits with initial positions shown in Table IV and orbits shown in Figure 12, where they are tracked for 200 turns. These orbits are tracked forward 60 million turns and then reversed and initial and final positions agree to 14 significant figures, except for trajectory C which is near a "stable fixed point" of the $\nu = 0.25$ resonance which obtains agreement to 21 significant digits. Figure 12 displays these results.

In Case B we have chosen $\nu_x = .245$ and $\nu_y = .12$, and $\Delta\nu = .01$. This case lies on the $\nu_x = 1/4$, $\nu_y = 1/8$ resonance. In the 60 million turns simulation of reference 1 a small increase in X-emittance coupled with a small decrease in y-emittance was observed. This change of less than 1% was comparable to statistical limits and an additional 60 million turns were simulated to investigate its possible significance.

Results of the full 120 million turn simulations are displayed in Table V and figure 14; over the full simulation there are no large changes in X,Y or R emittances.

Repeatability experiments were performed with four trajectories with initial positions $x = y = A\sigma$, $x' = y' = 0$ with $A = 0.5, 1.0, 1.5, 2.0$. Figures 15 and 16 show these trajectories in x,x' and y,y' phase planes; evidence of

the $\nu_x = .25$ and $\nu_y = .125$ resonances is clearly visible.

In figure 17 results of the repeatability experiments with A = 0.5, 1.0 and 2.0 are shown and agreement to 14 significant figures is obtained as in previous cases A and C above.

The fourth trajectory ($x_0 = 1.5\sigma$) failed the repeatability test and disagreement between initial and final trajectories is fully developed after only 30,000 turns (see Figure 18). The significance of this effect and its implifications for beam stability will be studied in a future note.

References

1. D. Neuffer, A. Riddiford and A. Ruggiero, Fermilab Note FN-333, April 1981.

2. D. Neuffer, A. Riddiford and A. Ruggiero, IEEE Trans. on Nuclear Science NS-28,p 2494 (1981).

3. P.R. Bevington, Data Reduction and Error Analysis for the Physical Sciences, McGraw-Hill Book Company (1969)

TABLE I. Emittance data for Case C: $\nu_x = 0.3439$; $\nu_y = 0.1772$; $\Delta\nu = 0.0100$
Cumulative values.

Real Ring Time (min)	Million turns	X_{av} (mm-mrad)	Doubling Time (days)	Y_{av} (mm-mrad)	Doubling Time (days)	R_{av} (mm-mrad)	Doubling Time (days)
$\frac{2}{3}$	2	0.0175496	-0.571	0.0187898	0.685	0.0257119	-28.7
$1\frac{1}{3}$	4	0.0175487	-3.95	0.0187970	0.984	0.0257165	2.36
2	6	0.0175462	-2.50	0.0187972	4.22	0.0257149	-16.9
$2\frac{2}{3}$	8	0.0175454	-3.11	0.0187962	-10.9	0.0257136	-5.04
$3\frac{1}{3}$	10	0.0175451	-4.93	0.0187957	-15.0	0.0257131	-7.71
4	12	0.0175453	-13.9	0.0187955	-16.0	0.0257131	-15.1
$4\frac{2}{3}$	14	0.0175463	22.2	0.0187963	36.2	0.0257143	28.5
$5\frac{1}{3}$	16	0.0175460	106.	0.0187966	26.3	0.0257143	41.5
6	18	0.0175444	-9.89	0.0187967	28.5	0.0257133	-34.5
$6\frac{2}{3}$	20	0.0175444	-13.7	0.0187969	22.3	0.0257135	-97.1
$7\frac{1}{3}$	22	0.0175442	-16.0	0.0187968	39.6	0.0257133	-64.5
8	24	0.0175449	-78.9	0.0187964	3510.	0.0257135	-169.
$8\frac{2}{3}$	26	0.0175453	106.	0.0187954	-20.4	0.0257130	-45.5
$9\frac{1}{3}$	28	0.0175443	-27.1	0.0187952	-20.6	0.0257122	-23.2
10	30	0.0175438	-18.4	0.0187952	-23.7	0.0257118	-20.8
$10\frac{2}{3}$	32	0.0175444	-46.1	0.0187957	-59.6	0.0257125	-52.2
$11\frac{1}{3}$	34	0.0175447	-367.	0.0187959	-222.	0.0257130	-269.
12	36	0.0175446	-109.	0.0187962	140.	0.0257131	-2510.
$12\frac{2}{3}$	38	0.0175443	-59.2	0.0187965	57.3	0.0257131	661.
$13\frac{1}{3}$	40	0.0175445	-127.	0.0187965	75.2	0.0257132	285.
14	42	0.0175443	-77.3	0.0187966	69.8	0.0257132	587.
$14\frac{2}{3}$	44	0.0175444	-109.	0.0187963	327.	0.0257130	-402.
$15\frac{1}{3}$	46	0.0175443	-102.	0.0187963	201.	0.0257130	-554.
16	48	0.0175442	-73.7	0.0187963	306.	0.0257129	-227.
$16\frac{2}{3}$	50	0.0175445	-562.	0.0187962	-1250.	0.0257130	-869.
$17\frac{1}{3}$	52	0.0175446	-1050.	0.0187964	165.	0.0257132	351.
18	54	0.0175442	-93.9	0.0187963	383.	0.0257129	-288.
$18\frac{2}{3}$	56	0.0175442	-94.0	0.0187966	121.	0.0257131	-2090.
$19\frac{1}{3}$	53	0.0175441	-99.7	0.0187967	99.4	0.0257131	1360.
20	60	0.0175441	-104.	0.0187966	131.	0.0257131	-3000.

TABLE II. Emittance data for Case C: $\nu_x = 0.3439$; $\nu_y = 0.1772$; $\Delta\nu = 0.0100$
Cumulative values.
Statistically significant doubling times.
Scatter values.

Real Ring Time (min)	Million turns	Statistically Significant Doubling Times X (days)	Y (days)	R (days)	Scatter Values SX (mm-mrad)	SY (mm-mrad)	SR (mm-mrad)
2	6	1.81	1.64	2.42	0.000212	0.000251	0.000234
4	12	5.08	4.63	6.77	0.000215	0.000252	0.000236
6	18	9.39	8.56	12.5	0.000213	0.000250	0.000235
8	24	14.4	13.2	19.2	0.000213	0.000251	0.000235
10	30	20.2	18.4	26.9	0.000214	0.000250	0.000235
12	36	26.5	24.2	35.3	0.000214	0.000251	0.000235
14	42	33.4	30.6	44.7	0.000214	0.000250	0.000234
16	48	40.7	37.2	54.6	0.000214	0.000251	0.000234
18	54	48.6	44.5	65.2	0.000214	0.000250	0.000234
20	60	56.9	52.2	76.4	0.000214	0.000250	0.000234

TABLE III. Emittance data for Case A; $\nu_x = \nu_y = 0.245$; $\Delta\nu = 0.010$
Cumulative values.

Real Ring Time (min)	Million turns	X_{av} (mm-mrad)	Doubling Time (days)	Y_{av} (mm-mrad)	Doubling Time (days)	R_{av} (mm-mrad)	Doubling Time (days)
$\frac{2}{3}$	2	0.0237166	0.3	0.0236805	-0.3	0.0336119	-1.5
$1\frac{1}{3}$	4	0.0237070	1.6	0.0236929	-2.5	0.0336144	1.9
2	6	0.0236984	-0.8	0.0236972	1.3	0.0336123	-6.7
$2\frac{2}{3}$	8	0.0237149	0.8	0.0236935	-3.1	0.0336211	2.0
$3\frac{1}{3}$	10	0.0237005	-2.0	0.0237146	.6	0.0336278	1.3
4	12	0.0237104	2.2	0.0237039	3.5	0.0336288	1.8
$4\frac{2}{3}$	14	0.0237044	-12.	0.0237051	3.9	0.0336267	4.1
$5\frac{1}{3}$	16	0.0237062	28.	0.0237028	41.	0.0336267	6.7
6	18	0.0237050	-21.	0.0237059	5.4	0.0336277	7.1
$6\frac{2}{3}$	20	0.0237085	6.3	0.0237017	-13.	0.0336277	9.2
$7\frac{1}{3}$	22	0.0236997	-3.5	0.0237084	4.1	0.0336267	22.
8	24	0.0237051	-170.	0.0237027	-23.	0.0336262	50.
$8\frac{2}{3}$	26	0.0237059	30.	0.0237036	-220.	0.0336272	25.
$9\frac{1}{3}$	28	0.0237055	92.	0.0237060	11.	0.0336286	14.
10	30	0.0237051	-330.	0.0237034	-83.	0.0336263	190.
$10\frac{2}{3}$	32	0.0237058	42.	0.0237015	-13.	0.0336256	-92.
$11\frac{1}{3}$	34	0.0237026	-13.	0.0237045	41.	0.0336256	-96.
12	36	0.0237030	-18.	0.0237047	36.	0.0336253	-67.
$12\frac{2}{3}$	38	0.0237054	58.	0.0237013	-15.	0.0336249	-50.
$13\frac{1}{3}$	40	0.0237024	-16.	0.0237028	-50.	0.0336243	-33.
14	42	0.0237038	-50.	0.0237011	-17.	0.0336241	-35.
$14\frac{2}{3}$	44	0.0237033	-36.	0.0237020	-30.	0.0336246	-58.
$15\frac{1}{3}$	46	0.0237033	-42.	0.0237019	-34.	0.0336244	-58.
16	48	0.0237014	-17.	0.0237024	-63.	0.0336232	-30.
$16\frac{2}{3}$	50	0.0237034	-83.	0.0236993	-13.	0.0336224	-23.
$17\frac{1}{3}$	52	0.0237011	-17.	0.0237018	-54.	0.0336226	-29.
18	54	0.0237035	-200.	0.0237003	-21.	0.0336230	-39.
$18\frac{2}{3}$	56	0.0237025	-46.	0.0237012	-38.	0.0336226	-36.
$19\frac{1}{3}$	58	0.0237020	-33.	0.0237018	-88.	0.0336226	-39.
20	60	0.0237020	-38.	0.0237022	-350.	0.0336229	-54.

TABLE III (continued)

Real Ring Time (min)	Million Turns	X_{av} (mm-mrad)	Doubling Time (days)	Y_{av} (mm-mrad)	Doubling Time (days)	R_{av} (mm-mrad)	Doubling Time (days)
$20\frac{2}{3}$	62	0.0237038	140.	0.0237006	-33.2	0.0336228	-54.1
$21\frac{1}{3}$	64	0.0237021	-46.6	0.0237027	164.	0.0336231	-78.5
22	66	0.0237024	-62.8	0.0237020	-302.	0.0336229	-74.1
$22\frac{2}{3}$	68	0.0237031	-286.	0.0237008	-44.4	0.0336225	-58.6
$23\frac{1}{3}$	70	0.0237020	-50.3	0.0237020	-279.	0.0336226	-68.0
24	72	0.0237026	-109.	0.0237026	170.	0.0336238	-986.
$24\frac{2}{3}$	74	0.0237035	214.	0.0237018	-177.	0.0336238	-692.
$25\frac{1}{3}$	76	0.0237038	119.	0.0237024	371.	0.0336244	212.
26	78	0.0237030	-295.	0.0237031	78.9	0.0336244	231.
$26\frac{2}{3}$	80	0.0237043	74.3	0.0237023	1354.	0.0336245	195.
$27\frac{1}{3}$	82	0.0237031	-507.	0.0237035	60.1	0.0336246	179.
28	84	0.0237034	678.	0.0237023	-1290.	0.0336240	-2600.
$28\frac{2}{3}$	86	0.0237024	-92.3	0.0237023	6280.	0.0336233	-158.
$29\frac{1}{3}$	88	0.0237031	-539.	0.0237020	-250.	0.0336235	-225.
30	90	0.0237029	-219.	0.0237028	175.	0.0336239	-1670.
$30\frac{2}{3}$	92	0.0237037	185.	0.0237018	-159.	0.0336240	-33100.
$31\frac{1}{3}$	94	0.0237022	-84.1	0.0237033	89.4	0.0336240	9620.
32	96	0.0237033	706.	0.0237023	-1030.	0.0336242	687.
$32\frac{2}{3}$	98	0.0237036	263.	0.0237022	-508.	0.0336242	610.
$33\frac{1}{3}$	100	0.0237032	-3410.	0.0237022	-632.	0.0336240	3430.
34	102	0.0237022	-89.1	0.0237023	-2210.	0.0336234	-253.
$34\frac{2}{3}$	104	0.0237023	-112.	0.0237012	-87.3	0.0336230	-136.
$35\frac{1}{3}$	106	0.0237018	-75.4	0.0237018	-214.	0.0336230	-147.
36	108	0.0237020	-90.4	0.0237019	-291.	0.0336230	-155.
$36\frac{2}{3}$	110	0.0237028	-396.	0.0237012	-93.1	0.0336230	-163.
$37\frac{1}{3}$	112	0.0237022	-124.	0.0237018	-277.	0.0336230	-180.
38	114	0.0237026	-228.	0.0237019	-313.	0.0336231	-233.
$38\frac{2}{3}$	116	0.0237026	-289.	0.0237022	2600.	0.0336236	-1095.
$39\frac{1}{3}$	118	0.0237027	-432.	0.0237020	-631.	0.0336234	-441.
40	120	0.0237024	-186.	0.0237024	639.	0.0336234	-422.

TABLE IV. Initial values for Figures 12, 13, 15-18.

LABEL	$X_o = Y_o$	$X'_o = Y'_o$
$\sigma/2$	0.04082 mm	0
D	0.05	0.025 mrad
σ	0.08165	0
C	0.105	0.0525
1.5σ	0.12247	0
B	0.145	0.0725
2σ	0.16330	0
A	0.2	0.1

TABLE V. Emittance data for Case B. $\nu_x = 0.245$; $\nu_y = 0.120$; $\Delta\nu = 0.010$ TABLE V
Cumulative values.

Real Ring Time (min)	Million Turns	X_{av} (mm-mrad)	Doubling Time (days)	Y_{av} (mm-mrad)	Doubling Time (days)	R_{av} (mm-mrad)	Doubling Time (days)
$\frac{2}{3}$	2	0.0227520	0.2	0.0192872	0.1	0.0298409	0.1
$1\frac{1}{3}$	4	0.0227605	0.7	0.0193705	0.1	0.0299023	0.1
2	6	0.0227589	1.5	0.0193918	0.1	0.0299149	0.3
$2\frac{2}{3}$	8	0.0227293	-0.3	0.0193824	0.6	0.0298863	-0.8
$3\frac{1}{3}$	10	0.0227243	-0.4	0.0193464	-0.3	0.0298592	-0.4
4	12	0.0227275	-1.3	0.0193089	-0.2	0.0298374	-0.4
$4\frac{2}{3}$	14	0.0227243	2.0	0.0193784	-0.2	0.0298298	-0.5
$5\frac{1}{3}$	16	0.0227431	2.8	0.0192687	-0.2	0.0298235	-0.6
6	18	0.0227731	0.5	0.0192616	-0.3	0.0298419	-2.5
$6\frac{2}{3}$	20	0.0227619	1.1	0.0192598	-0.4	0.0298323	-1.5
$7\frac{1}{3}$	22	0.0227764	0.8	0.0192621	-0.5	0.0298447	37.
8	24	0.0227892	0.6	0.0192630	-0.7	0.0298550	3.1
$8\frac{2}{3}$	26	0.0228057	0.5	0.0192650	-1.0	0.0298687	1.5
$9\frac{1}{3}$	28	0.0228304	0.4	0.0192609	-1.0	0.0298850	1.0
10	30	0.0228423	0.4	0.0192612	-1.3	0.0298944	0.9
$10\frac{2}{3}$	32	0.0228507	0.4	0.0192610	-1.5	0.0299007	1.0
$11\frac{1}{3}$	34	0.0228483	0.5	0.0192603	-1.7	0.0298985	1.3
12	36	0.0228320	1.0	0.0192638	-2.6	0.0298883	2.2
$12\frac{2}{3}$	38	0.0228238	1.5	0.0192628	-2.8	0.0298814	4.2
$13\frac{1}{3}$	40	0.0228216	1.9	0.0192602	-2.6	0.0298782	7.2
14	42	0.0228252	1.9	0.0192582	-2.5	0.0298796	6.9
$14\frac{2}{3}$	44	0.0228277	1.9	0.0192593	-3.2	0.0298822	5.7
$15\frac{1}{3}$	46	0.0228280	2.2	0.0192599	-3.9	0.0298828	6.0
16	48	0.0228312	2.1	0.0192581	-3.6	0.0298841	6.0
$16\frac{2}{3}$	50	0.0228347	1.9	0.0192597	-4.9	0.0298878	4.8
$17\frac{1}{3}$	52	0.0228339	2.4	0.0192654	-26.	0.0298908	4.2
18	54	0.0228401	1.9	0.0192605	-6.7	0.0298924	4.2
$18\frac{2}{3}$	56	0.0228499	1.5	0.0192590	-5.9	0.0298990	3.3
$19\frac{1}{3}$	58	0.0228554	1.5	0.0192570	-5.1	0.0299019	3.1
20	60	0.0228630	1.3	0.0192567	-5.4	0.0299076	2.7

TABLE V (continued)

Real Ring Time (min)	Million Turns	X_{av} (mm-mrad)	Doubling Time (days)	Y_{av} (mm-mrad)	Doubling Time (days)	R_{av} (mm-mrad)	Doubling Time (days)
$20\frac{2}{3}$	62	0.0228672	1.3	0.0192580	-7.2	0.0299115	2.6
$21\frac{1}{3}$	64	0.0228724	1.3	0.0192597	-11.0	0.0299167	2.4
22	66	0.0228687	1.5	0.0192553	-5.8	0.0299110	3.2
$22\frac{2}{3}$	68	0.0228658	1.8	0.0192529	-5.0	0.0299072	4.2
$23\frac{1}{3}$	70	0.0228660	2.0	0.0192506	-4.4	0.0299058	5.0
24	72	0.0228666	2.1	0.0192479	-3.9	0.0299045	5.9
$24\frac{2}{3}$	74	0.0228645	2.5	0.0192450	-3.5	0.0299011	8.6
$25\frac{1}{3}$	76	0.0228599	3.3	0.0192422	-3.2	0.0298957	21.1
26	78	0.0228599	3.5	0.0192396	-3.0	0.0298940	38.2
$26\frac{2}{3}$	80	0.0228646	3.1	0.0192380	-3.0	0.0298966	19.5
$27\frac{1}{3}$	82	0.0228682	2.8	0.0192374	-3.1	0.0298989	13.9
28	84	0.0228650	3.5	0.0192350	-3.0	0.0298950	36.3
$28\frac{2}{3}$	86	0.0228694	3.1	0.0192336	-3.0	0.0298974	20.3
$29\frac{1}{3}$	88	0.0228664	3.8	0.0192321	-3.0	0.0298942	68.8
30	90	0.0228648	4.4	0.0192288	-2.8	0.0298908	-55.6
$30\frac{2}{3}$	92	0.0228633	5.1	0.0192278	-2.8	0.0298890	-30.0
$31\frac{1}{3}$	94	0.0228636	5.3	0.0192293	-3.2	0.0298902	-50.3
32	96	0.0228650	5.2	0.0192317	-3.9	0.0298929	216.
$32\frac{2}{3}$	98	0.0228660	5.2	0.0192327	-4.4	0.0298942	61.8
$33\frac{1}{3}$	100	0.0228656	5.7	0.0192341	-5.0	0.0298948	50.1
34	102	0.0228661	5.9	0.0192342	-5.4	0.0298952	44.2
$34\frac{2}{3}$	104	0.0228686	5.3	0.0192352	-6.2	0.0298978	23.5
$35\frac{1}{3}$	106	0.0228703	5.1	0.0192357	-6.8	0.0298995	18.9
36	108	0.0228711	5.2	0.0192379	-8.9	0.0299014	15.2
$36\frac{2}{3}$	110	0.0228697	5.9	0.0192391	-10.9	0.0299011	16.8
$37\frac{1}{3}$	112	0.0228706	5.9	0.0192429	-24.0	0.0299043	12.4
38	114	0.0228705	6.3	0.0192445	-46.9	0.0299052	12.0
$38\frac{2}{3}$	116	0.0228687	7.5	0.0192463	+985.	0.0299050	12.9
$39\frac{1}{3}$	118	0.0228668	9.2	0.0192462	-801.	0.0299034	16.0
40	120	0.0228629	14.7	0.0192472	+93.5	0.0299012	23.0

Figure 1. Resonance lines up to 13th order which cross the area in tune space used by Case C: $\nu_x = 0.3439$, $\nu_y = 0.1772$, $\Delta\nu = 0.0100$

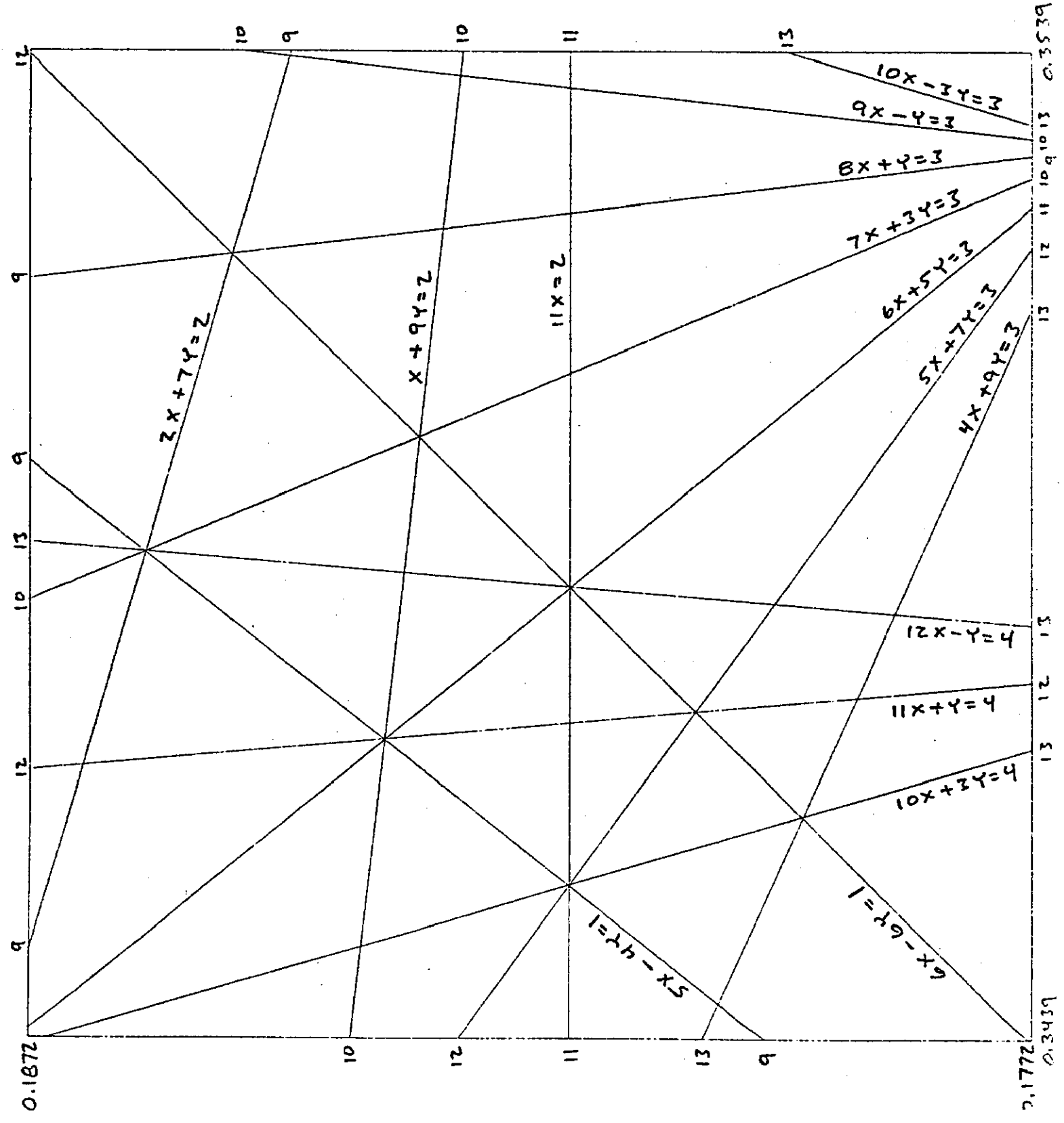

Figure 2. Tune space showing the limits of Case C and how close the corners come to the undesirable lines of order 3, 6 and 8.

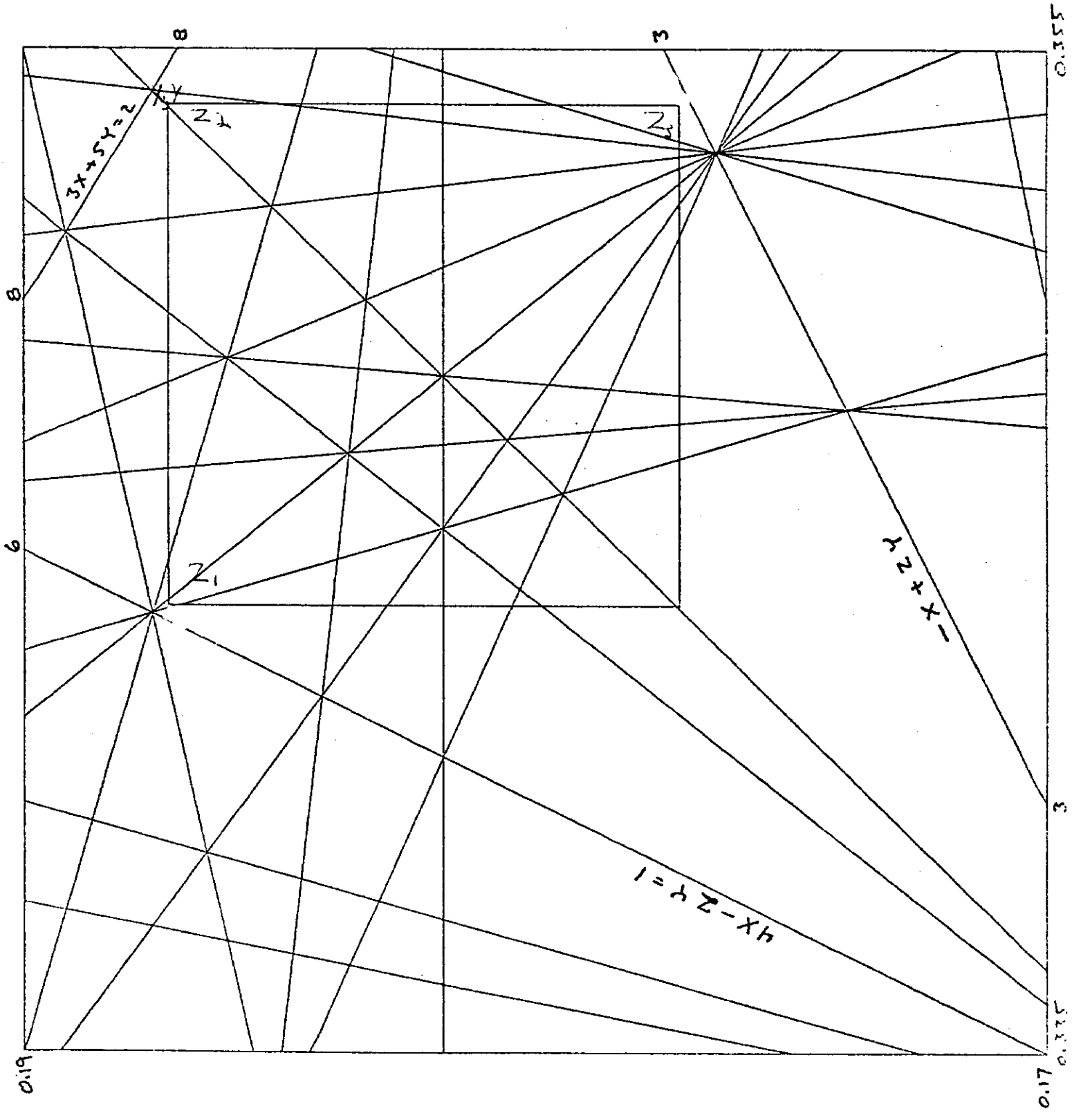

Figure 3. Summary of emittance variations. Each bar represents 100 emittance values.
Case C: $\nu_x = 0.3439$, $\nu_y = 0.1772$, $\Delta\nu = 0.0100$

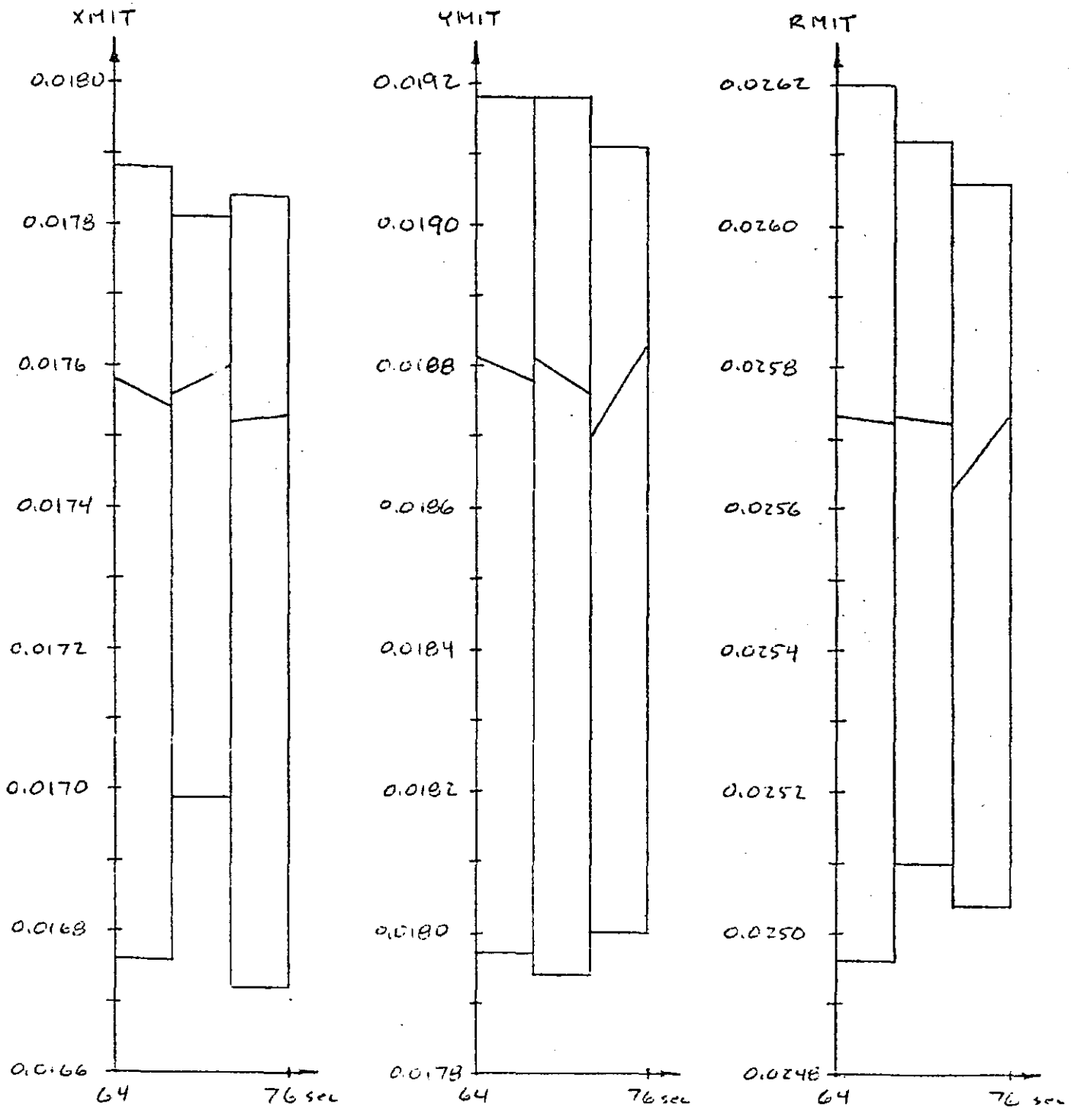

Figure 4. Comparison of X-emittance cumulative doubling times with statistically significant doubling times.
Case C: $\nu_x = 0.3439$, $\nu_y = 0.1772$, $\Delta\nu = 0.0100$

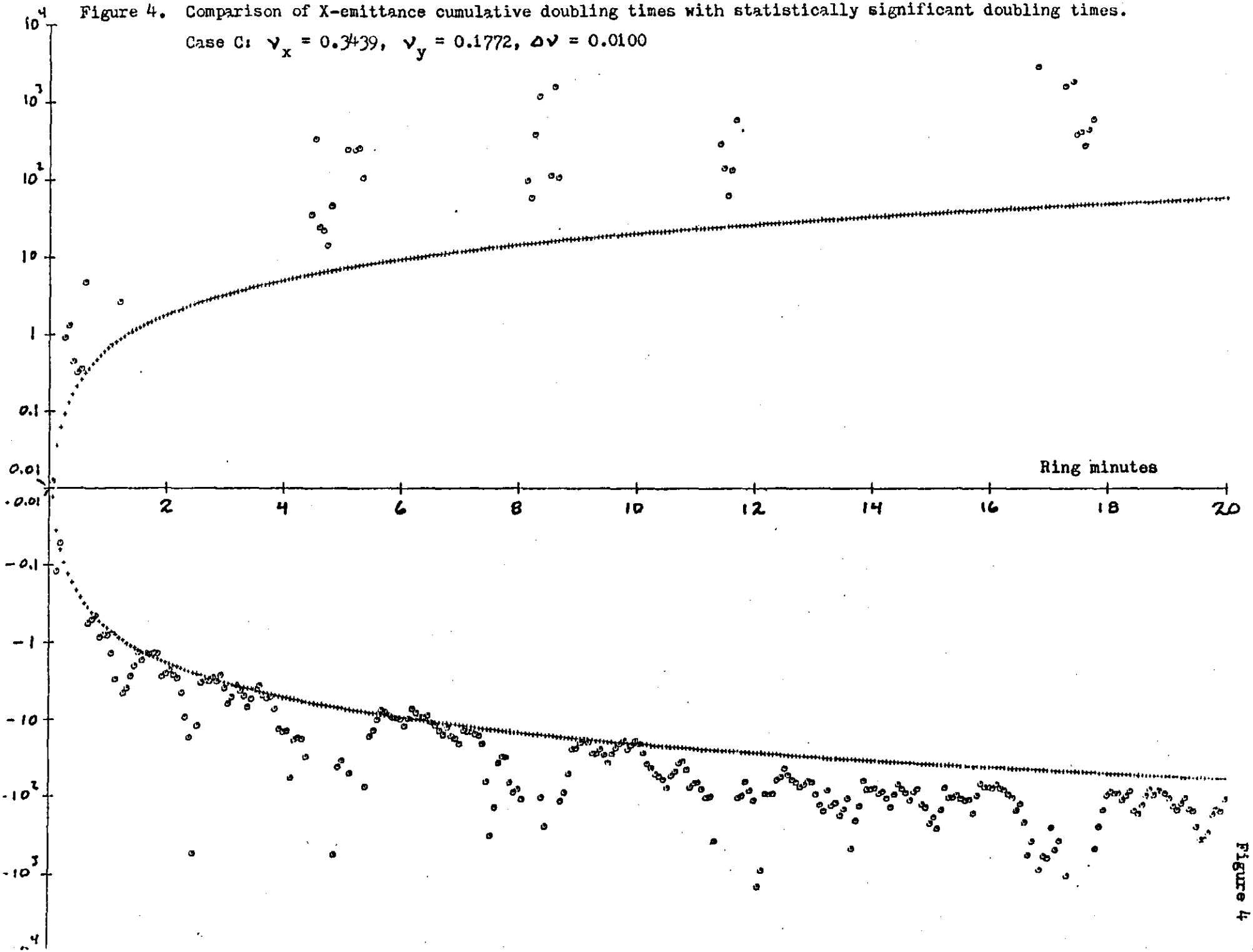

Figure 4

Figure 5. Comparison of Y-emittance cumulative doubling times with statistically significant doubling times.
Case C: $\nu_x = 0.3439$, $\nu_y = 0.1772$, $\Delta\nu = 0.0100$

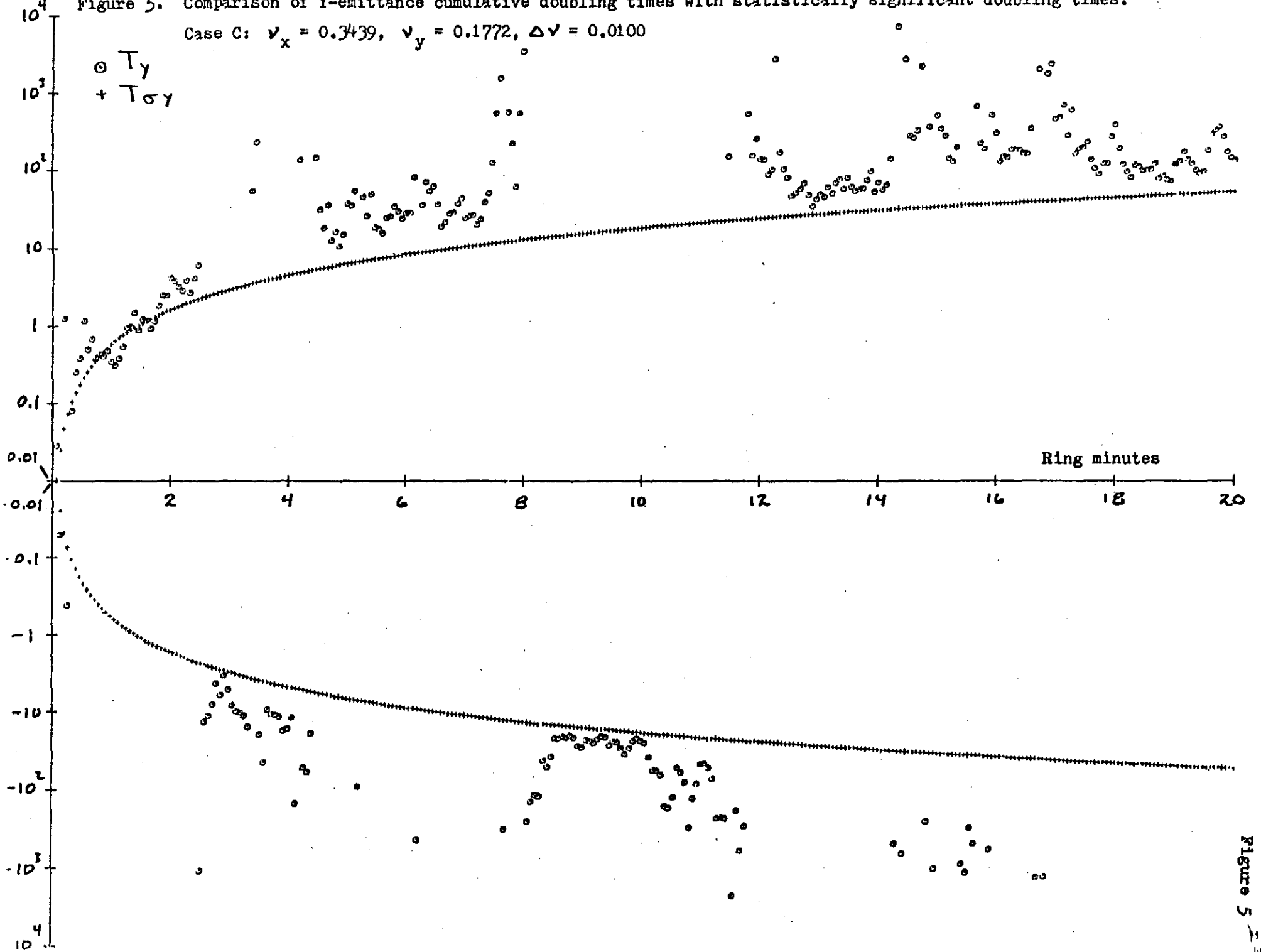

Figure 5

Figure 6. Comparison of R-emittance cumulative doubling times with statistically significant doubling times.
Case C: $\nu_x = 0.3439$, $\nu_y = 0.1772$, $\Delta\nu = 0.0100$

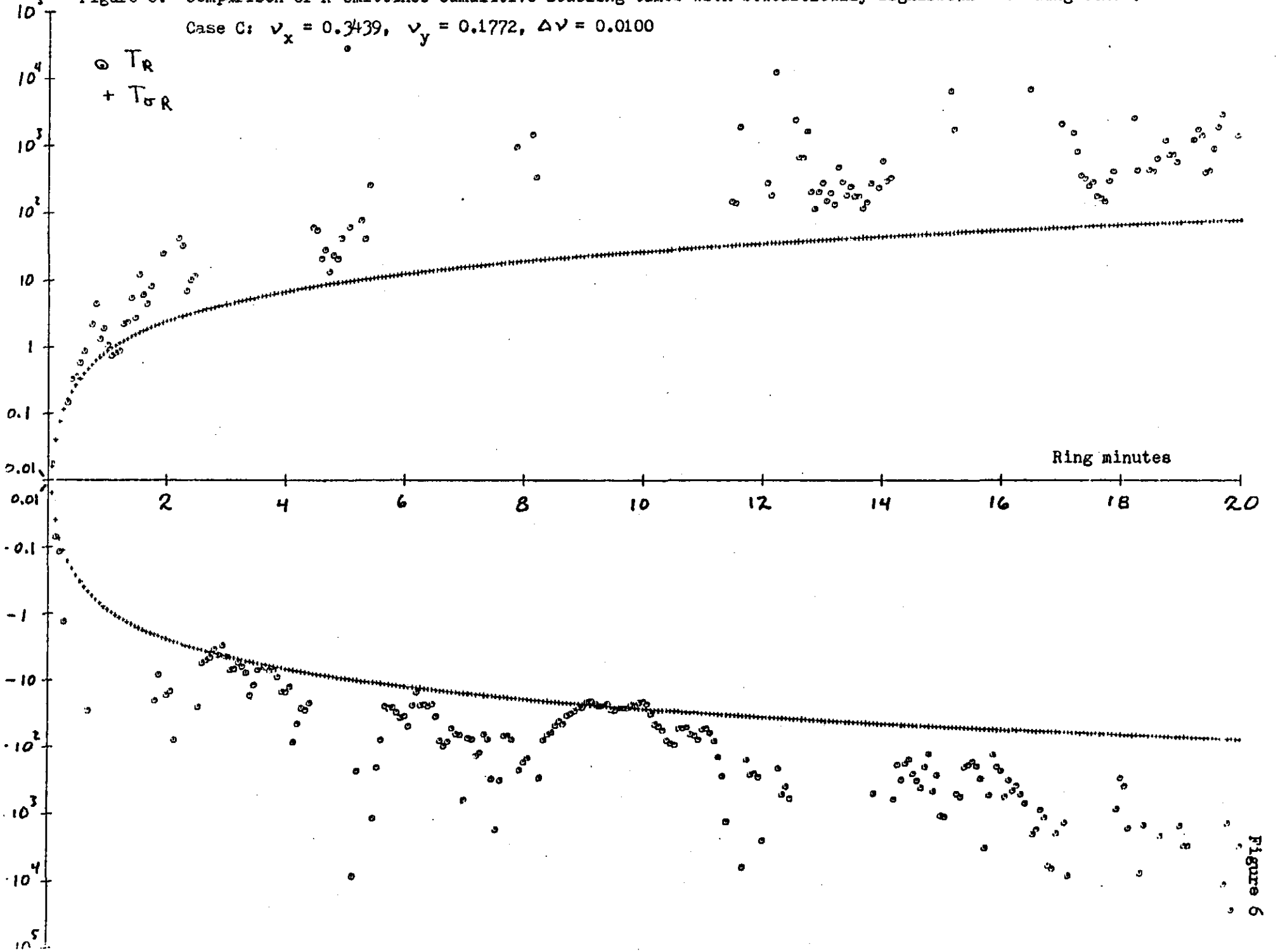

Figure 6

Figure 7. Double precision repeatability Experiment.
Case C: $\nu_x = 0.3439$, $\nu_y = 0.1772$, $\Delta\nu = 0.0100$
Initial conditions: $X = A\sigma$, where $\sigma = 0.08165$mm.
$X' = Y = 0$, $Y' = 0.1559$mrad.

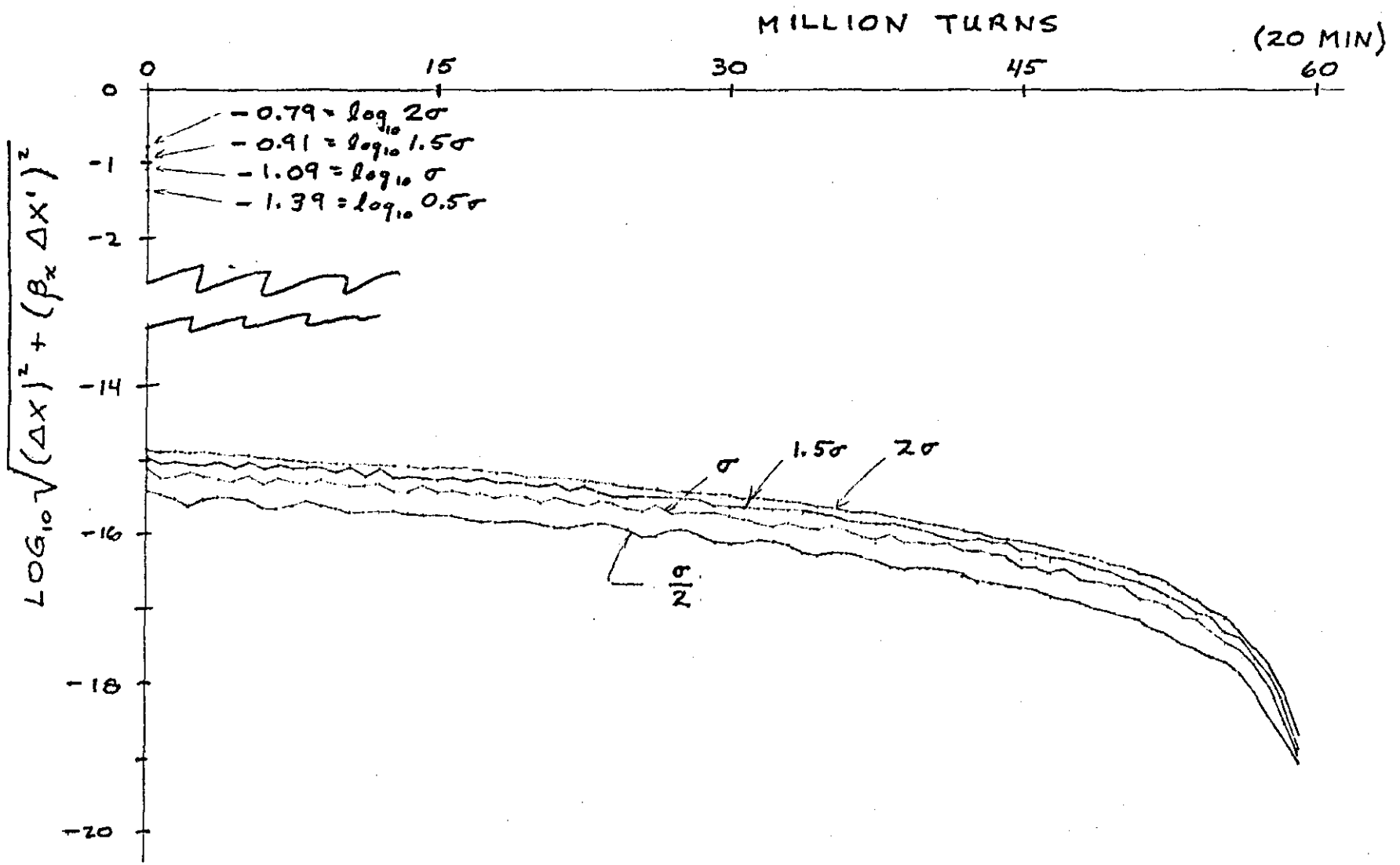

Figure 7

Figure 8. (X,X') phase space. 400 points in each of the four orbits used in the repeatability experiment. (See Figure 7)

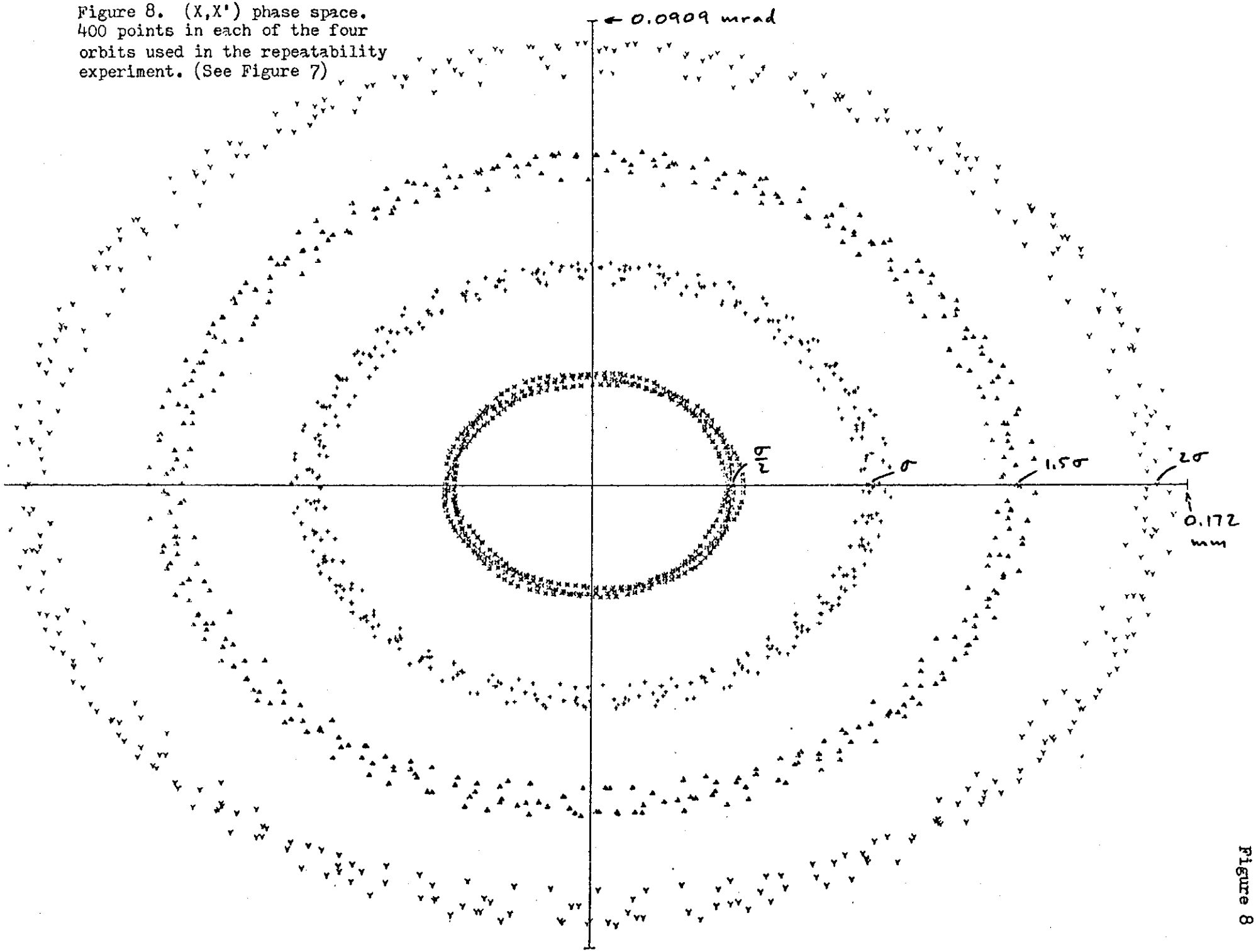

Figure 8

Figure 9. (X,X') phase space. 41 orbits.
X = 0.03, 0.06, ... , 1.20 & 0.17mm.
X' = Y = 0, Y' = 0.1559mrad.

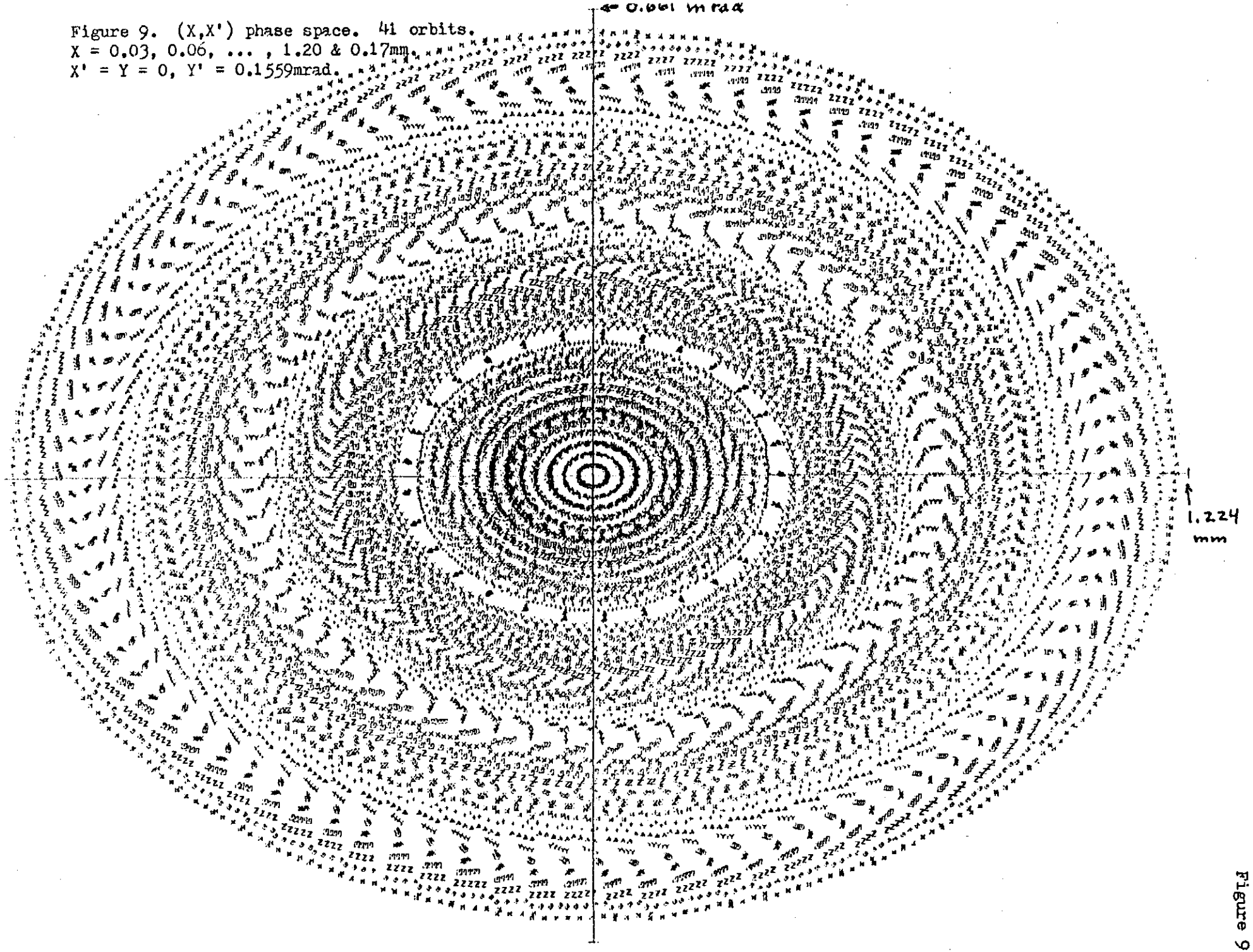

Figure 9

Figure 10. (X,X') phase plane. 40 orbits.

X = 0.03, 0.06, ... , 1.20 mm

X' = Y = 0, Y' = $\beta\sigma$

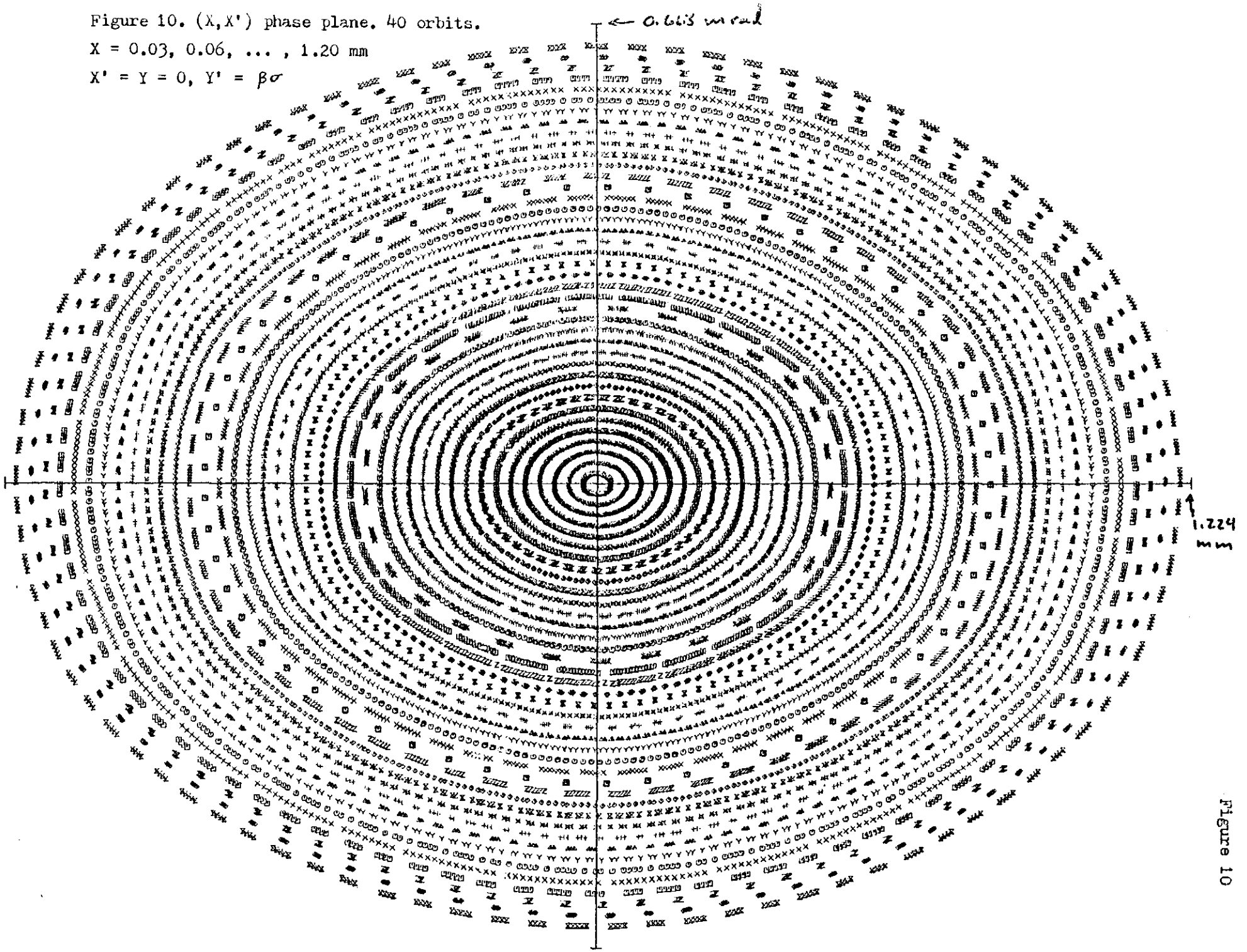

Figure 10

Figure 11. Statistically significant doubling times (dashed lines) compared with doubling times for Case A. $\nu_x = \nu_y = 0.245$, $\Delta\nu = 0.010$ Note logarithmic scales. Points within the dashed lines are significantly different from zero.

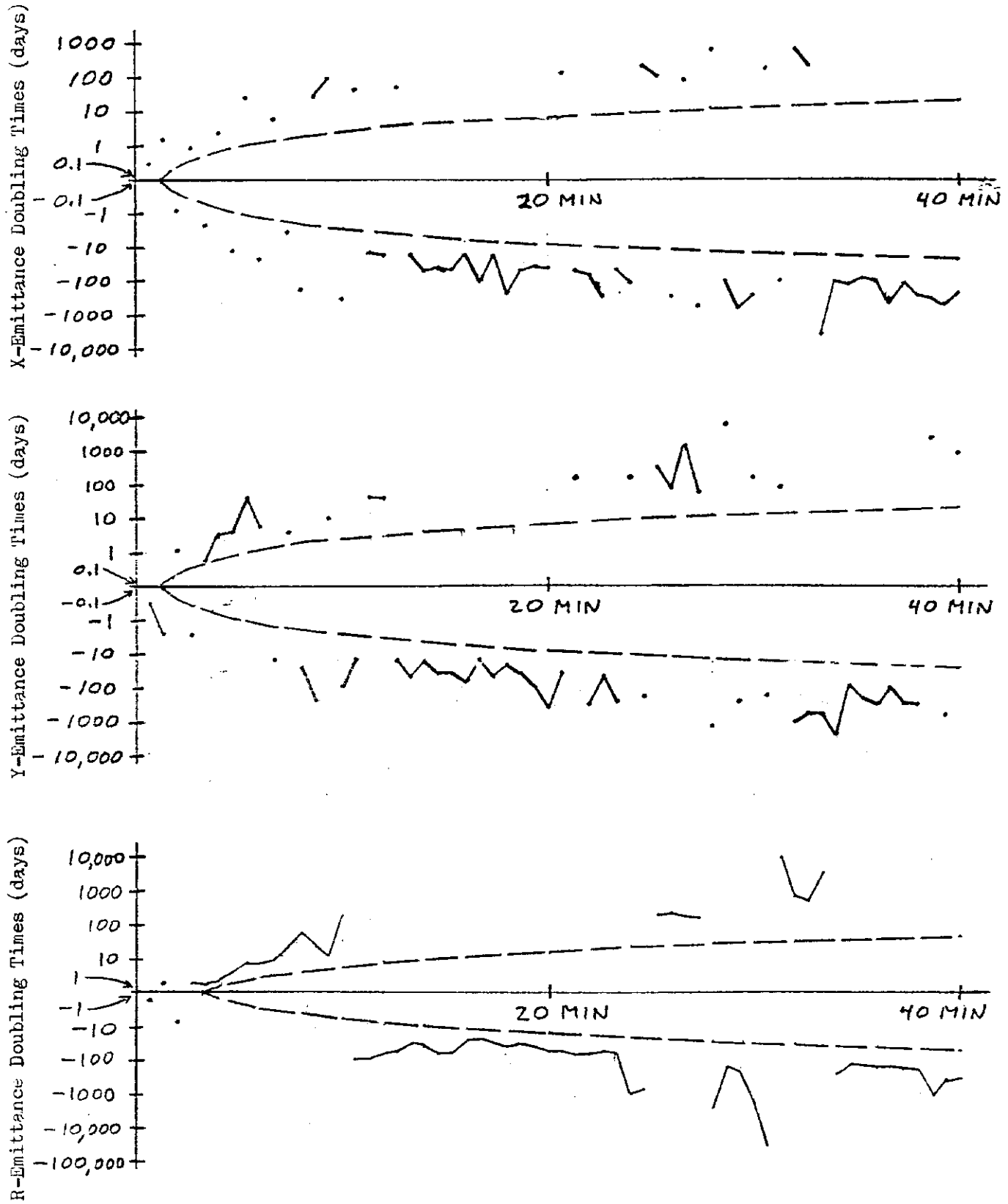

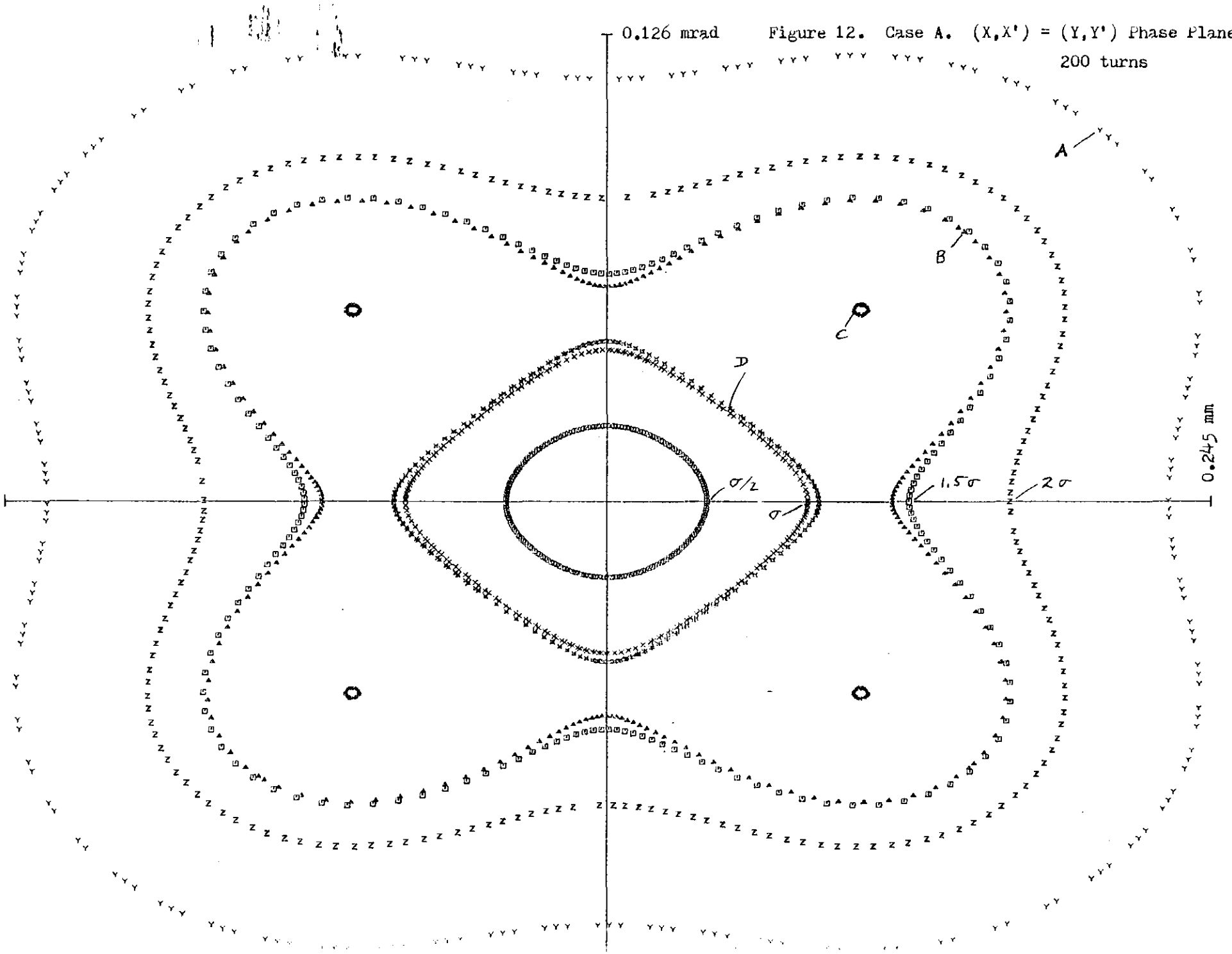

Figure 12. Case A. (X,X') = (Y,Y') Phase Plane
200 turns

Figure 12

Figure 13

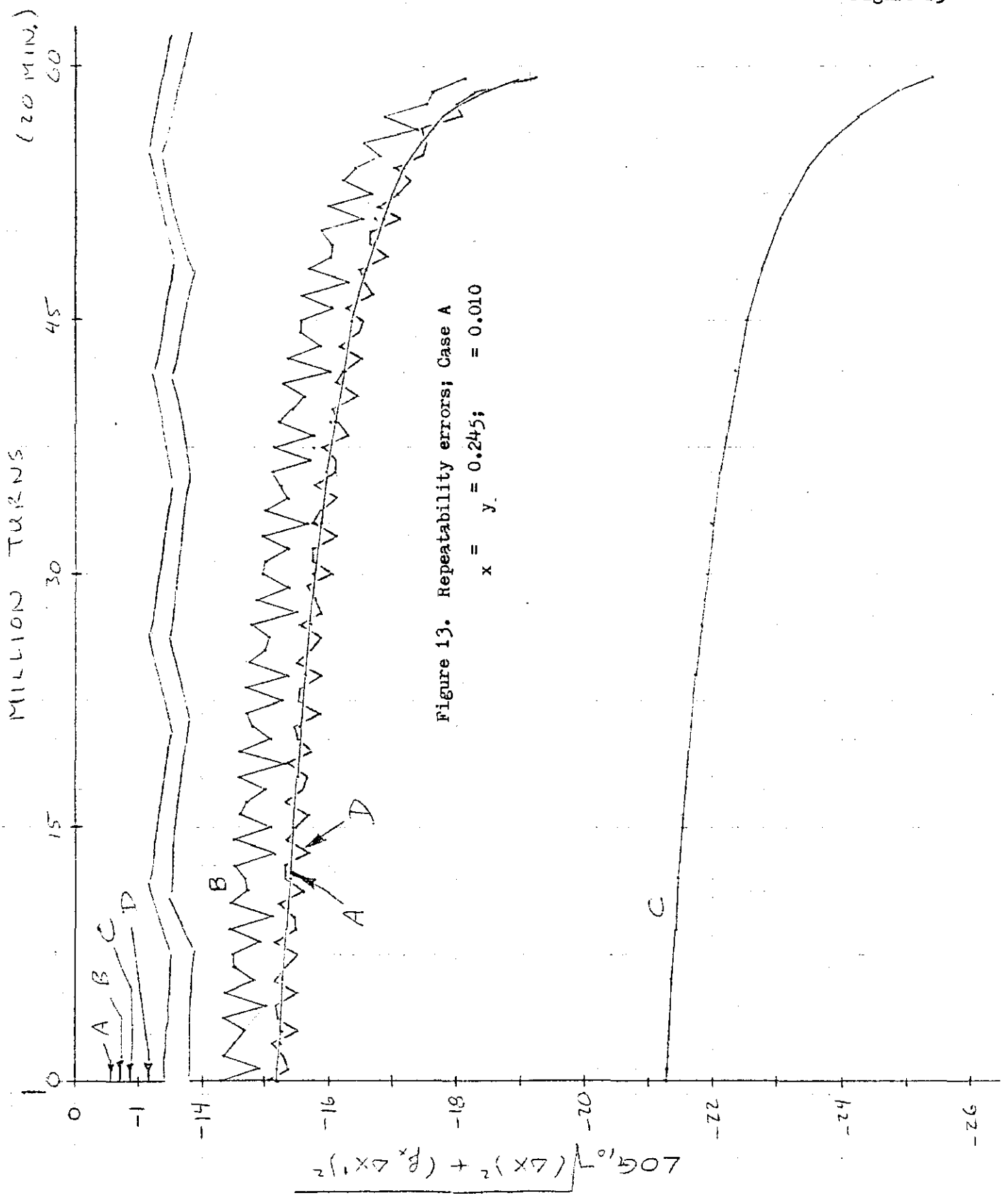

Figure 13. Repeatability errors; Case A

$x = y = 0.245$; $= 0.010$

Figure 14. Statistically significant doubling times (dashed lines) compared with doubling times for Case B. $\nu_x = 0.245$, $\nu_y = 0.120$, $\Delta\nu = 0.010$

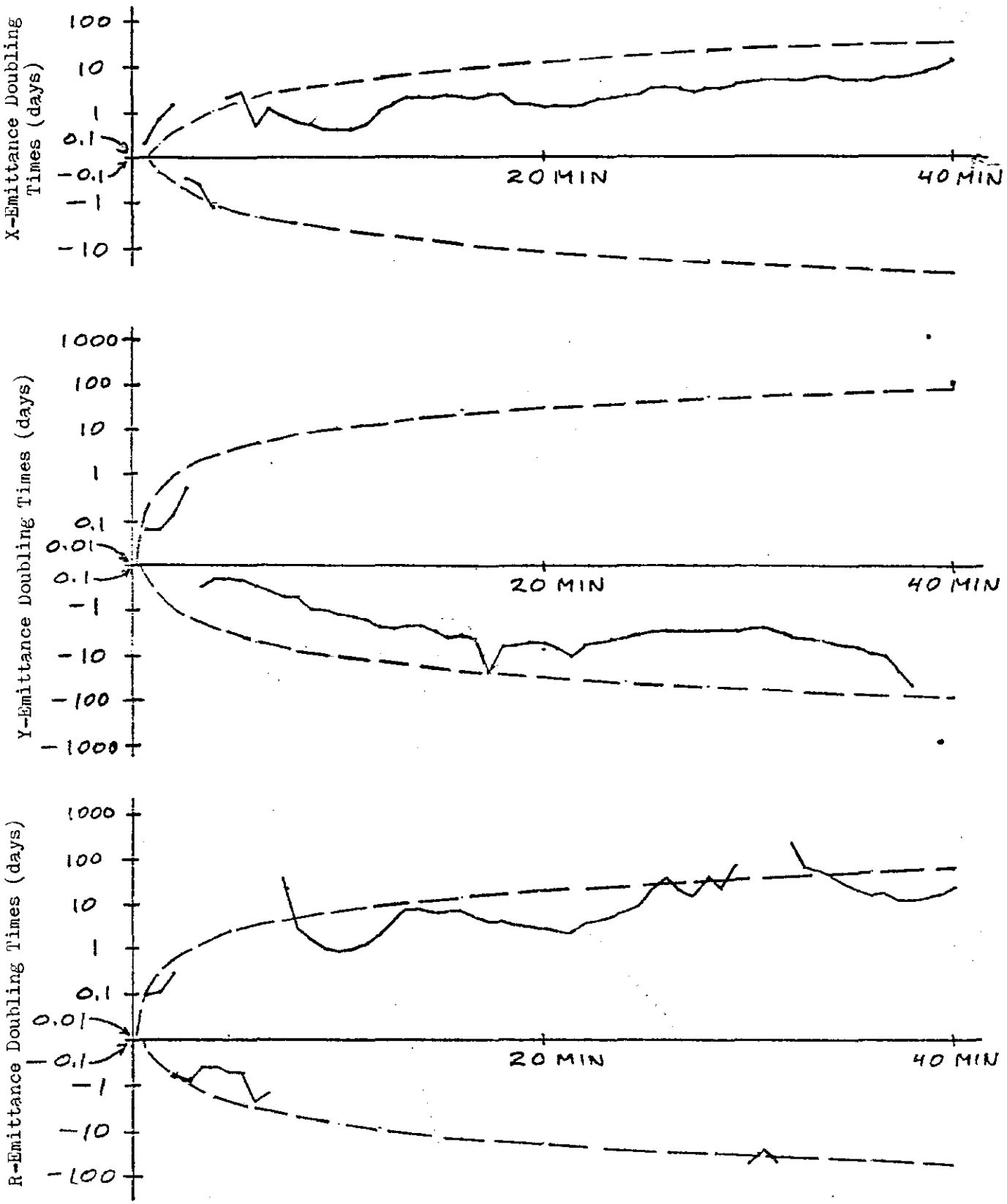

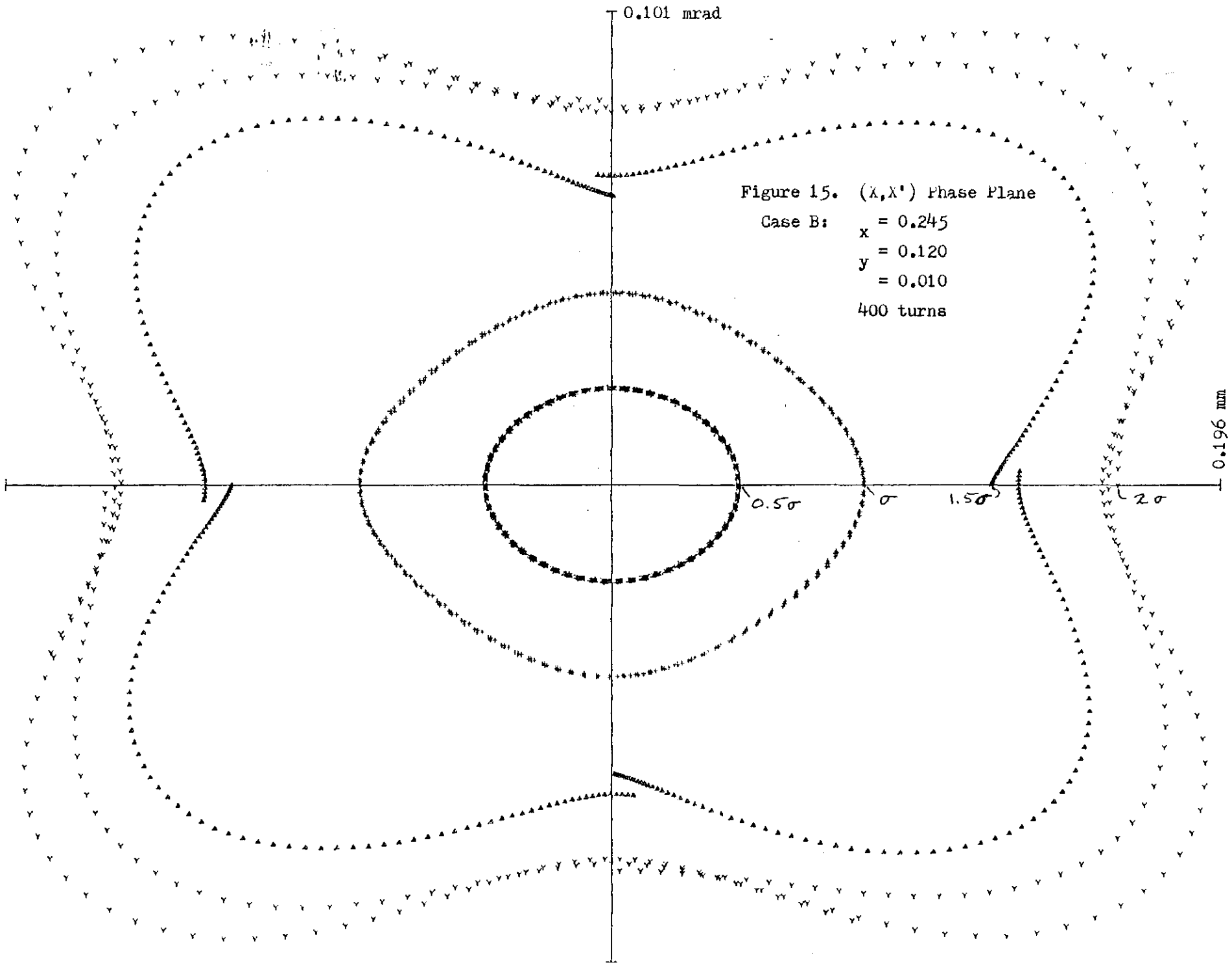

Figure 15. (X,X') Phase Plane
Case B: $\nu_x = 0.245$
$\nu_y = 0.120$
$\nu_s = 0.010$
400 turns

Figure 15

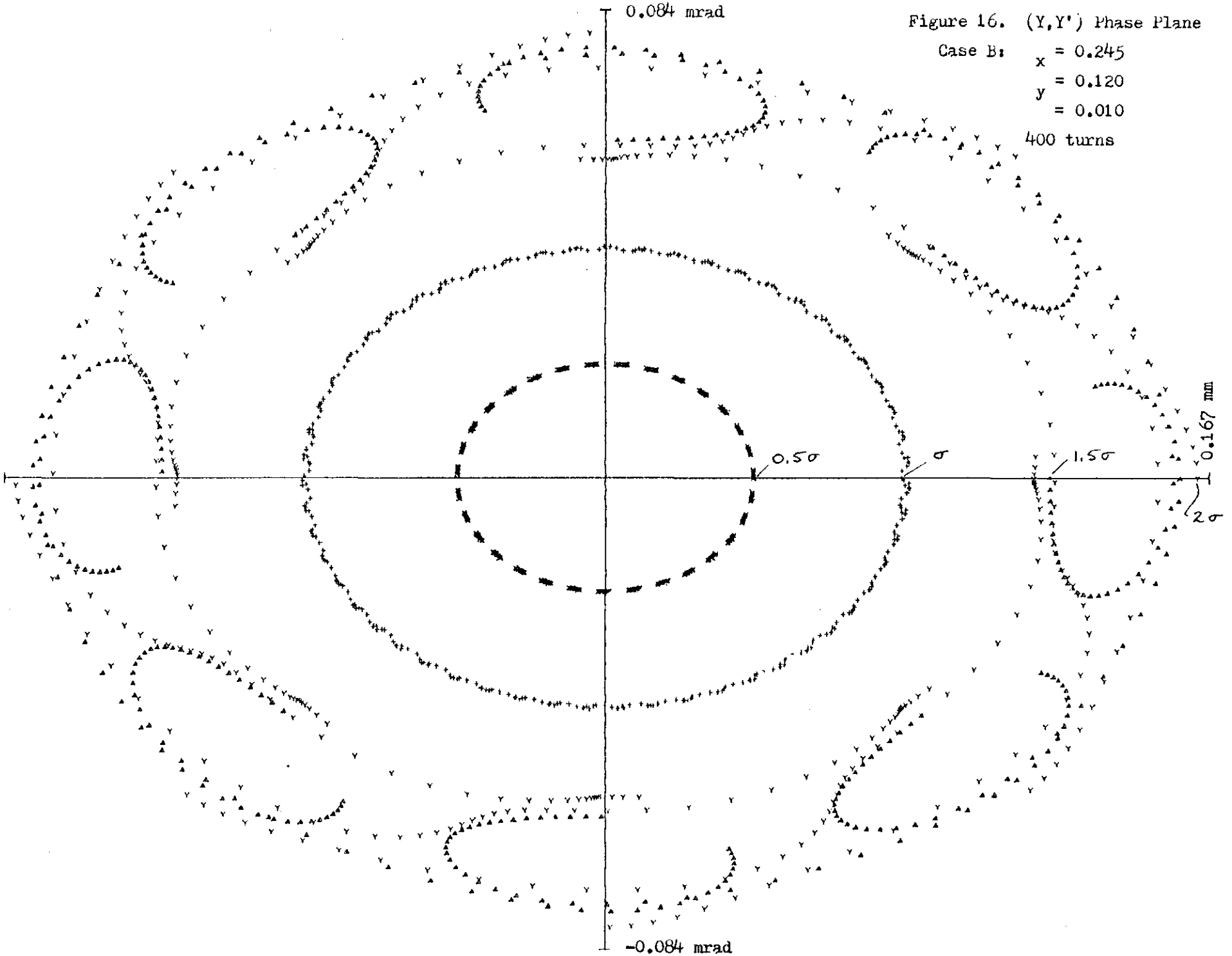

Figure 16. (Y,Y') Phase Plane
Case B: $\nu_x = 0.245$
$\nu_y = 0.120$
400 turns

Figure 16

Figure 17. Repeatability errors; Case B: $\nu_x = 0.245$; $\nu_y = 0.120$; $\Delta\nu = 0.010$
Initial Conditions; $X'_o = Y'_o = 0$
$X_o = Y_o = A\sigma$, where A = 0.5, 1.0, 2.0 and where $\sigma = 0.08165$ mm

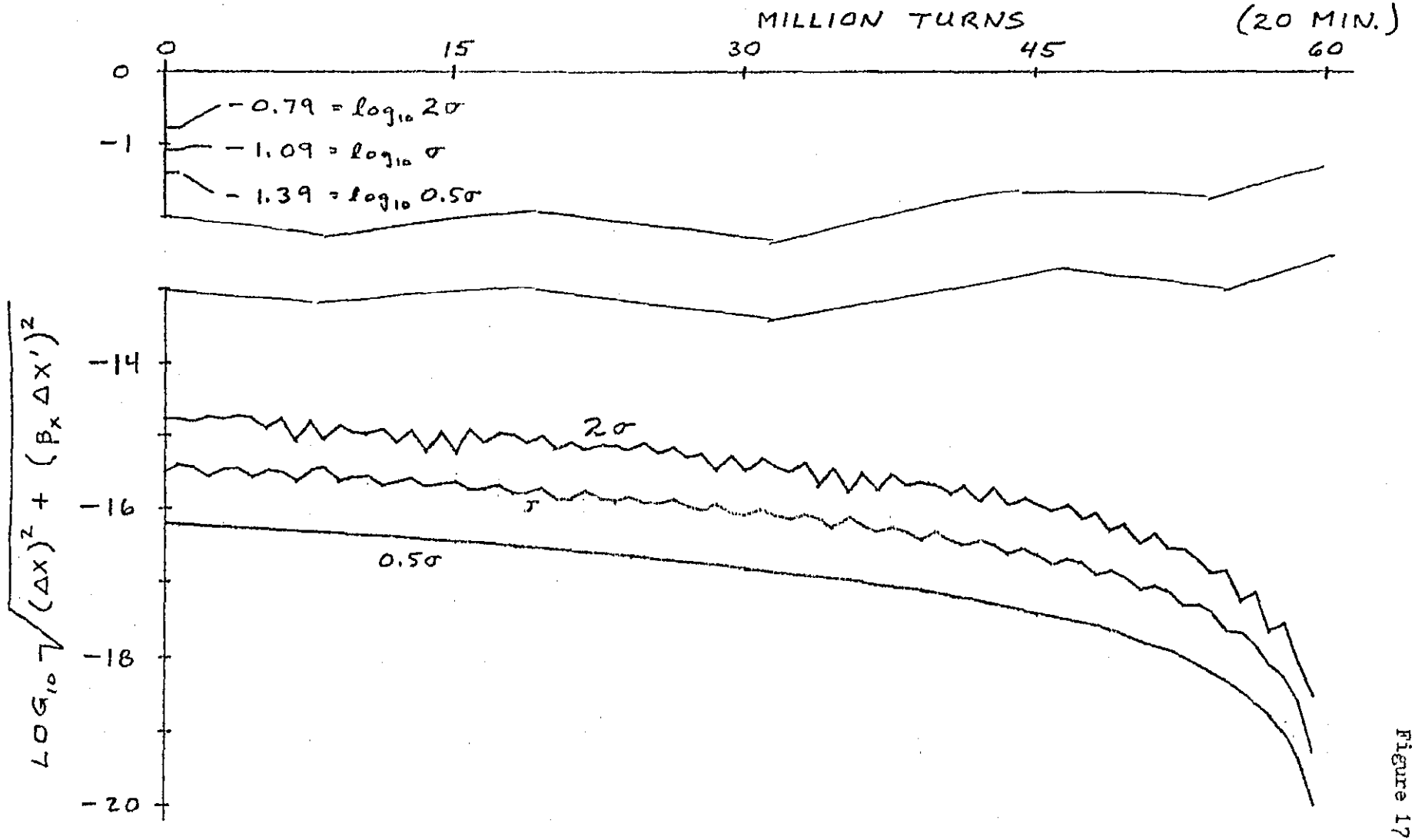

Figure 17

Figure 18. Repeatability errors; Case B: $\nu_x = 0.245$; $\nu_y = 0.120$; $\Delta\nu = 0.010$
Initial Conditions: $X_o = Y_o = 1.5\sigma = 0.1225$ mm; $X'_o = Y'_o = 0$

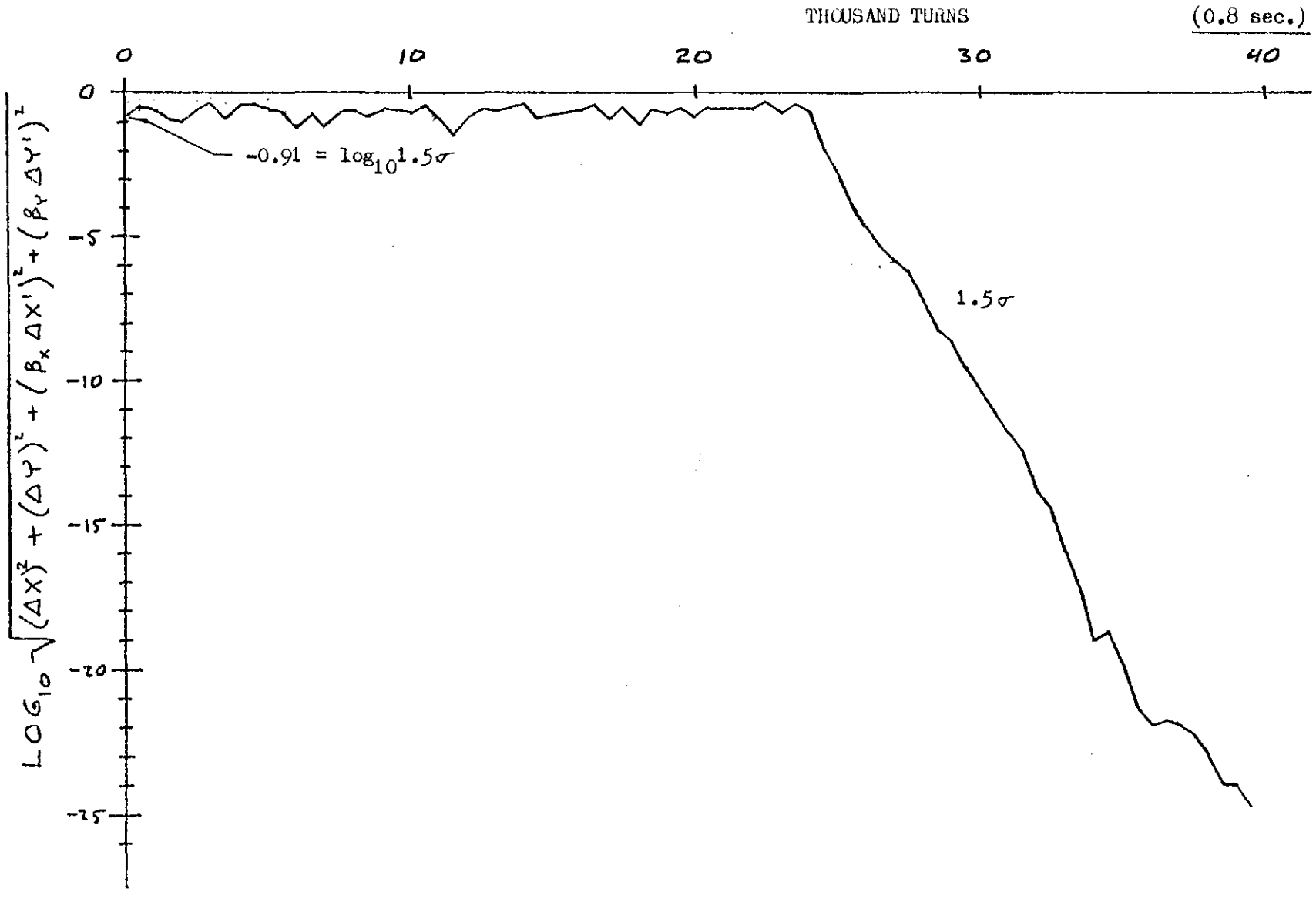

Figure 18